

Three-dimensional in vivo analysis of *Dictyostelium* mounds reveals directional sorting of prestalk cells and defines a role for the myosin II regulatory light chain in prestalk cell sorting and tip protrusion

Patricia A. Clow¹, Tung-Ling L. Chen², Rex L. Chisholm² and James G. McNally^{3,*}

¹Department of Biology, Washington University, Box 1229, St Louis, Missouri 63130, USA

²Department of Cell and Molecular Biology, Northwestern University Medical School, 303 E. Chicago Avenue, Chicago, Illinois 60611, USA

³Laboratory of Receptor Biology and Gene Expression, Division of Basic Sciences, National Cancer Institute, Building 41, Room C615, 41 Library Drive MSC 5055, Bethesda, Maryland 20892-5055, USA

*Author for correspondence (e-mail: mcnallyj@exchange.nih.gov)

Accepted 4 April; published online 23 May 2000

SUMMARY

During cell sorting in *Dictyostelium*, we observed that GFP-tagged prestalk cells (ecmAO-expressing cells) moved independently and directionally to form a cluster. This is consistent with a chemotaxis model for cell sorting (and not differential adhesion) in which a long-range signal attracts many of the prestalk cells to the site of cluster formation. Surprisingly, the ecmAO prestalk cluster that we observed was initially found at a random location within the mound of this Ax3 strain, defining an intermediate sorting stage not widely reported in *Dictyostelium*. The cluster then moved en masse to the top of the mound to produce the classic, apical pattern of ecmAO prestalk cells. Migration of the cluster was also directional, suggesting the presence of another long-range guidance cue. Once at the mound apex, the cluster continued moving upward leading to protrusion of the mound's tip. To investigate the role of the cluster in tip protrusion, we examined ecmAO prestalk-cell

sorting in a myosin II regulatory light chain (RLC) null in which tips fail to form. In RLC-null mounds, ecmAO prestalk cells formed an initial cluster that began to move to the mound apex, but then arrested as a vertical column that extended from the mound's apex to its base. Mixing experiments with wild-type cells demonstrated that the RLC-null ecmAO prestalk-cell defect is cell autonomous. These observations define a specific mechanism for myosin's function in tip formation, namely a mechanical role in the upward movement of the ecmAO prestalk cluster. The wild-type data demonstrate that cell sorting can occur in two steps, suggesting that, in this Ax3 strain, spatially and temporally distinct cues may guide prestalk cells first to an initial cluster and then later to the tip.

Key words: *Dictyostelium*, Morphogenesis, Cell movement, Myosin, Prestalk cell

INTRODUCTION

Pattern formation via cell rearrangements is a common process during development. Such cell sorting may occur via long-range guidance signals, cell-cell adhesion, or both. Nerve growth cones appear to recognize their final target through cell adhesion molecules like fasciclin III (Kose et al., 1997), connectin (Nose et al., 1997) or neurotactin (Speicher et al., 1998), while longer range signals may initially be provided by chemoattractants such as netrin (Keynes and Cook, 1995). Long-range signals are also important for the migration of sex myoblasts in *Caenorhabditis elegans* (Burdine et al., 1997) (Chen and Slaughter, 1998) and tracheal cells in *Drosophila* (Sutherland et al., 1996; Krasnow, 1997) where, in both cases, a role for fibroblast growth factor is implicated. An alternative role for adhesion in cell sorting is via differential adhesion, where cells segregate into distinct populations based on their relative adhesive strengths (Steinberg and Poole, 1981). A long

history of in vitro studies has demonstrated the feasibility of this model (Steinberg, 1962, 1970; Nose et al., 1988; Steinberg and Takeichi, 1994), with more recent in vivo evidence supplied by the sorting of the oocyte in the *Drosophila* follicle (Godt and Tepass, 1998).

Regardless of the signals that control it, cell sorting requires cell movement and cell shape changes, which in turn depend on the interaction of many cytoskeletal proteins. A key cytoskeletal component, myosin II, which has now been found to play important roles in morphogenesis in several systems. Myosin II is required at multiple steps during *Drosophila* development (Edwards and Kiehart, 1996) where it appears to serve several different functions depending on the specific morphogenetic process. For example, in *Drosophila* oogenesis, border cell migration may require myosin II for amoeboid locomotion, whereas centripetal cell migration may utilize myosin II to induce a purse string contraction of a cell sheet. A comparable role may be served by myosin II in

embryonic elongation in *C. elegans* where RNA interference of the myosin II regulatory light chain prevents elongation of the embryo into a worm shape (Shelton et al., 1999). This gross morphological defect is accompanied by a failure of hypodermal cells to elongate properly, suggesting that myosin II is normally involved in these morphogenetic cell shape changes.

Much work has also been devoted to understanding both the mechanism of cell sorting and the role of myosin II in *Dictyostelium discoideum*. This organism provides an excellent experimental system in which to study the molecular basis of cell movement in a multicellular mass. Signal transduction pathways (Aubry and Firtel, 1999) and the actin/myosin cytoskeleton (Uyeda and Titus, 1997; Noegel and Schleicher, in press) are well studied in *Dictyostelium*, and therefore provide a framework for understanding the integration of these two morphogenetic components. *Dictyostelium* undergoes morphogenesis (Gross, 1994; Loomis, 1996) with cells differentiating into two basic cell types (spore and stalk) accompanied by a series of morphological changes, one of which is the formation of a nipple-like structure called the tip on top of a flattened hemisphere of cells called the mound. As determined from cell-type-specific β -galactosidase markers, *Dictyostelium* cell types are initially scattered and then sort out into spatially distinct populations at the mound stage. The prestalk cells segregate to the mound tip and a thin layer at the mound base, while prespore cells occupy the remainder of the mound (Williams et al., 1989; Haberstroh and Firtel, 1990; Escalante and Loomis, 1995; Early et al., 1995). This segregation of cell types is known to require myosin II (Traynor et al., 1994), but myosin II's specific function in this process is unknown. Still less is known about the mechanisms underlying the protrusion of the tip, although mounds of myosin II null cells fail to form this structure. More generally, the mechanisms by which prestalk and prespore cells sort in *Dictyostelium* are unknown, but competing models for both differential adhesion and chemotaxis have been proposed.

Support for sorting via differential adhesion in *Dictyostelium* comes from several studies. According to this model, random motion drives cell segregation because of adhesive preferences, much like the separation into two phases of a mixture of oil and water. Such a sorting process should exhibit 'clumpy' intermediate stages, as observed by Feinberg et al. (1979). These investigators dissociated prestalk and prespore cells from mounds, labeled the cells and then allowed them to reaggregate. They found that the two cell types formed many small, distinct clusters at first, and then progressively fewer, but larger clusters, completely analogous to the patterns of sorting predicted by differential adhesion. Other studies have suggested that prestalk and prespore cells exhibit the requisite differences in adhesion. Compared to prestalk cells, prespore cells have a higher concentration of discoidin-I (Lam et al., 1981), a carbohydrate-binding protein with an RGD motif. The two cell types may also differ in levels of a cell-surface glycoprotein, gp150; antibodies directed against this protein more effectively dissociated prespore cells taken from slugs compared to prestalk cells (Lam et al., 1981). When prespore and prestalk cells taken from slugs were allowed to reaggregate, the same antibodies prevented cell sorting (Siu et al., 1983).

Support for sorting via chemotaxis in *Dictyostelium* comes

from a variety of sources. When dissociated slug cells are allowed to reaggregate, prestalk cells move directionally to a central region in the mound (Takeuchi et al., 1988). Studies of cell motion during the formation of secondary tips in slugs (induced either by removing the primary tip or exposing slugs to caffeine) have shown that prestalk cells move directionally into newly forming slug tips (Durstion and Vork, 1979; Zimmermann and Siegert, 1998), raising the possibility that similar directional motion could be instrumental in mound tip formation. Directional sorting in the mound could be mediated by cAMP, as much evidence indicates that prestalk cells are more chemotactic towards cAMP than prespore cells (Matsukuma and Durston, 1979; Sternfeld and David, 1981; Wang and Schaap, 1985; Mee et al., 1986; Early et al., 1995). Further evidence demonstrates that exogenous cAMP can override normal prestalk sorting patterns. When mounds are placed on a substratum containing cAMP, prestalk cells migrate to the mound periphery, instead of the tip (Matsukuma and Durston, 1979). When the comparable experiment is performed with a mutant that overexpresses cAMP phosphodiesterase, prestalk cells migrate to the entire base of the mound (Traynor et al., 1992). In this same mutant in the absence of exogenous cAMP, prestalk cells eventually collect at the mound tip (Traynor et al., 1992), but this sorting is much slower than normal.

Most of the observations in *Dictyostelium* that support differential adhesion, or alternatively, chemotaxis to cAMP are based on perturbations of the normal sorting process, or other indirect evidence. It is not known how sorting actually occurs in vivo, but these alternative models do make distinctive predictions about how cells should move in the mound. The differential adhesion model predicts that prestalk and prespore cells should move randomly and collect into progressively larger clusters, analogous to the observations of Feinberg et al. (1979) when they mixed these two cell types and allowed them to reaggregate. The chemotaxis model predicts that prestalk cells should move directionally and independently to the mound apex. To date these predictions have not been directly tested, because studies of cell sorting in the *Dictyostelium* mound have been based on static analyses using β -galactosidase driven by cell-type-specific promoters. Such analyses do not permit in vivo observation of how cells actually move during the sorting process, and they also may miss transient intermediate stages in the sorting process, such as are predicted to occur during differential adhesive sorting.

To distinguish between these alternative models for sorting in *Dictyostelium*, we have used time-lapse three-dimensional (3D) microscopy to examine in vivo sorting of prestalk or prespore cells marked with green fluorescent protein (GFP) in a common laboratory strain Ax3. In this study, we have examined in vivo sorting of a class of prestalk cells defined by the full-length ecmAO promoter. This class (hereafter referred to as ecmAO prestalk cells) is localized according to the classical prestalk pattern, namely at the mound tip and slug anterior (Jermyn and Williams, 1991; Williams et al., 1989; Loomis, 1996). Our in vivo studies show that, in Ax3, ecmAO prestalk cells sort directionally and independently to form a cluster, consistent with a model for chemotactic sorting rather than differential adhesive sorting. The initial cluster forms at a random position in the mound and then elongates as it moves directionally to the mound apex. Once there, the elongated

cluster continues moving upward leading to tip protrusion. Having elucidated this sorting process and its association with tip formation, we then investigated myosin II's role. We show here that upward movement of the ecmAO cluster into the mound tip is a myosin II-dependent process that requires the mechanical function of the myosin regulatory light chain, thereby offering a specific mechanism for myosin's role in cell sorting and tip formation.

MATERIALS AND METHODS

Cell lines and culture conditions

The following *Dictyostelium discoideum* cell lines were used, described in the order of their appearance in the Results section: Ax3 expressing green fluorescent protein (GFP) under the control of the ecmAO or psA promoter (referred to here as ecmAO-GFP and psA-GFP respectively) (Chen et al., 1998); myosin II regulatory light chain null (RLC⁻) (Chen et al., 1994); RLC⁻ expressing GFP under the control of the ecmAO or psA promoter (referred to here as RLC⁻ ecmAO-GFP and RLC⁻ psA-GFP, respectively) (Chen et al., 1998); Ax3 (Loomis, 1971) as a wild-type axenic strain. All cell lines were grown at 21°C in HL-5 medium (Spudich, 1982) in 100 mm-diameter plastic Petri plates. Ax3 psA-GFP and RLC⁻ psA-GFP were maintained with 10 µg/ml geneticin selection. Ax3 ecmAO-GFP and RLC⁻ ecmAO-GFP were maintained with 80 µg/ml geneticin selection. Cells were starved by harvesting, centrifugation, and washing in phosphate buffer (5.7 mM K₂HPO₄, 17.0 mM KH₂PO₄, 2.0 mM MgSO₄·7H₂O, 0.2 mM CaCl₂·2H₂O, 0.34 mM dihydrostreptomycin sesquisulfate salt) (Clark et al., 1980, DeLozanne and Spudich, 1987).

Microscopy

Cells were allowed to settle onto a dialysis membrane laid on a coverslip kept in a humid chamber. To create chimeras, two different cell lines were mixed prior to settling on the dialysis membrane. To image the side view of tipped mounds and fingers, cells were allowed to settle onto 2% agar, an agar block was excised, and then the block was laid on a coverslip in a humid chamber such that the lens imaged the side of the structure. Imaging set-up and collection were performed as described in Doolittle et al. (1995). We recorded images from a custom-modified IMT-2 Olympus inverted microscope with a scientific-grade CCD camera cooled to -40°C.

Time-lapse 3D fluorescence microscopy

To follow cell sorting, we used 3D time-lapse fluorescence microscopy. Imaging was begun when the cells reached the appropriate developmental stage. Depending on the magnification and resolution desired for imaging, we used either an Olympus S Plan PL 0.3 NA/10× air lens, an Olympus LWD CD Plan PL 0.4 NA/20× air lens, an Olympus D Plan Apo UV 0.7 NA/20× air lens, an Olympus D Plan Apo UV 0.8 NA/20× oil immersion lens, or a Leitz NPL Fluotar 1.3 NA/40× oil immersion lens. For each lens, z step size was set equal to xy resolution of the CCD camera, thereby yielding 3D imaging at comparable resolution in x, y and z. Typically, 32 or 64 focal planes were collected per time point, depending on the height of the specimen. An exposure time of 30-200 milliseconds per focal plane was used with a 50-95% neutral density filter in the light path of a 100 W mercury arc lamp or 150 W xenon arc lamp. 3D images were acquired at 2-30 minute intervals. A typical experiment had 30 timepoints.

Bright-field microscopy

Bright-field images were collected using the lenses listed above. An exposure time of 20-50 milliseconds was used with a halogen lamp.

Cell viability

The following precautions were taken to insure cell viability. First, after an imaging experiment, cell chambers were observed up to 1 day later to confirm that development proceeded properly. Second, the rate of development was compared in cell chambers on and off the microscope, and found to be the same. Third, to reduce light exposure to a specimen, timepoints were spaced more widely or 2D imaging was performed instead of 3D imaging. In either case, cell movements were consistent with those observed under increased light exposure. Finally, to verify that transitions in cell motile behavior were not due to imaging, data collection was sometimes started after the transition occurred to demonstrate that light exposure did not induce the transition.

Image processing

Recorded 3D images were processed to reduce out-of-focus light by several different well-characterized restoration methods (Preza et al., 1992; Conchello and McNally, 1996; see Doolittle et al. (1995) and McNally et al. (1994) for a detailed discussion of these methods and their validation.

Quantification of cell motion

3D cell tracking was performed using an upgraded version of customized software (Awasthi et al., 1994). To determine the directionality or randomness of cell motion into an ecmAO prestalk cluster, we performed an analysis of cell trajectories designed to determine if prestalk cells exhibited directional movement specifically associated with cluster formation. During the period of ecmAO cell sorting, virtually all cells rotate vigorously. To factor out the contribution of rotational motion, we asked whether the ecmAO prestalk cells exhibited radially inward directional motion to form the prestalk cluster. At each timepoint, the center of mass of a cluster was calculated by averaging coordinates for all tracked cells entering the cluster. This center of mass at each timepoint was then subtracted from the trajectory coordinates at that timepoint to remove the effects of drift or rotational motion of the cluster. In this coordinate system, the origin now defined a fixed cluster location and the motion of cells toward or away from the cluster could be examined. To assess if cells entered the cluster directionally, we computed the number of steps that a cell moved either toward or away from the cluster. This was done by first transforming the modified cell coordinates to a polar coordinate system. Changes in a cell's radial coordinate were then used to define either inward or outward motion (i.e. a decrease in a cell's radial coordinate over a single timepoint was defined as an inward step toward the cluster, and vice versa). For all cells examined, the number of inward steps versus the total number of steps within a 3-minute interval were tallied. The null hypothesis for random cell movement is that the number of inward steps is 50% of the total steps. This was tested for each 3-minute interval by using the Gaussian approximation to the binomial probability (Snedecor and Cochran, 1980). Sufficiently small probabilities indicate that the motion is unlikely to be random.

RESULTS¹

ecmAO prestalk cells form a cluster that migrates to the mound apex and becomes the tip

To examine prestalk-cell sorting in the mound, we used time-lapse 3D microscopy to image motion of cells expressing GFP under the control of the prestalk-cell marker ecmAO (full-length promoter) (71 different mounds examined). This

¹Timelapse movies of ecmAO and psA sorting in normal and RLC-null cell mounds are available at the author's web site (<http://rex.nci.nih.gov/RESEARCH/basic/lrbe/prestalkmov.html>) or on CDROM by request.

construct was an accurate reporter of ecmAO expression; its temporal and spatial expression patterns mirrored those previously observed with other ecmAO reporter constructs (Williams et al., 1989). In particular, an initially scattered distribution of ecmAO-GFP cells was observed in early mounds (Fig. 1A, top view; B, side view). Later, ecmAO-GFP cells became localized to the tips of mounds and slugs (Fig. 1F,G, side views). We could also occasionally detect a hint of the very earliest distribution reported for prestalk cells, namely a peripheral staining around the mound perimeter (Early et al., 1995) (see for example Fig. 5C). However, this pattern was not detectable in every mound, perhaps because of the well-known delay in acquisition of GFP fluorescence (Heim et al., 1994), or because ecmAO expression itself is very low at this early stage. In any event, all subsequent ecmAO patterns previously seen with β -galactosidase or other static markers were consistently reproduced by GFP expression, thereby enabling us to follow the evolution of a scattered distribution of ecmAO prestalk cells to a localized cluster in the mound tip.

By *in vivo* 3D imaging of ecmAO-GFP cells in the mound, we have observed intermediate stages in the spatial pattern of ecmAO prestalk expression not widely reported. Specifically, we found that, within every mound examined, the initially scattered distribution of ecmAO-GFP cells was followed by the formation of a cluster of ecmAO-GFP cells that was initially not at the mound apex or tip, but eventually migrated to the

apex and became the tip. (See Fig. 4 for a schematic and quantification of the different sorting stages that we observed.) The ecmAO prestalk cluster was first apparent as a small number of cells (<10) which was joined by progressively more cells to form an aggregate that was ultimately 1/4 to 1/3 the diameter of the mound (Figs 1C, top view; 2A, side view). Sometimes a cluster formed, but then disintegrated only to be replaced by a new cluster at another location (data not shown). The initial site of a cluster was random.

Eventually after a stable prestalk cluster emerged, it migrated upward over a period of 12–40 minutes toward the mound apex and, eventually, reached the mound apex (Fig. 1E). Upward migration of the cluster continued and the tip protruded (Fig. 1F,G). During the period of upward migration to the mound apex, the cluster often elongated to form either comma-shaped structures (Fig. 1D, top-down view of a mound) or columnar structures (Fig. 2B,C, side views of a mound). Time-lapse movies of cluster migration suggested that this elongation of the cluster arose, at least in part, due to the movement of more labeled cells into the cluster. In some mounds, these clusters eventually elongated into full-fledged spirals (Fig. 2E,F, stereo pair). These curved structures are probably due to the vigorous clockwise or counterclockwise rotation of mound cells that occurs in this Ax3 strain. Such spiral clusters of prestalk cells have been reported previously using β -galactosidase expression driven by either a partial ecmAO promoter (Early et al., 1995) or another prestalk enriched marker, RasD (Esch and Firtel, 1991).

Regardless of the cluster's precise structure, tip formation did not occur until the cluster reached the top of the mound (Figs 1E, 2C,D, side views). As the tip protruded upward, it was always stained with GFP-expressing cells. Other ecmAO prestalk cells were found in the cluster extending beneath the tip, although eventually all of the cells in the cluster condensed into the tip as it elongated to form a slug (e.g. Fig. 1G). Even at this stage, however, a small number of GFP-expressing cells were found scattered throughout the mound base.

Prespore cell distributions are largely complementary to ecmAO prestalk cell patterns

We also used time-lapse 3D microscopy to examine cells expressing GFP under the control of the prespore-cell marker psA (32 different mounds examined). Again, this construct was an accurate reporter of psA prespore expression: psA-GFP cells were initially scattered in early mounds (Fig. 3A, top view; B, side view) and were excluded from the tip in later mounds (Fig. 3G–I, top views), consistent with what had been observed for this (Williams et al., 1989) and other prespore markers (Haberstroh and Firtel, 1990).

Once again, our 3D *in vivo* analysis revealed intermediate stages of psA prespore

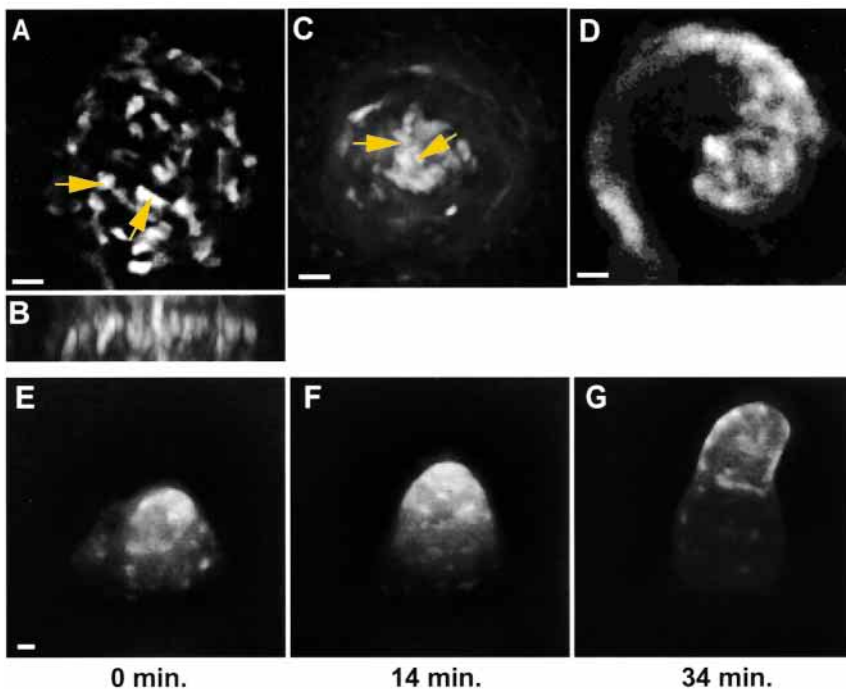


Fig. 1. Intermediate stages of ecmAO-GFP sorting in mounds. (A,B) Initial scattered distribution of ecmAO-GFP cells (two individual cells are indicated by arrows) in an early mound (A, top view (xy); B, side view (xz)). (C) Top view of a different mound after the initial cluster of ecmAO-GFP cells has formed. Two individual cells within the cluster are indicated by arrows. The mound periphery is about the width of the panel, and can be faintly seen from the dimly labeled cells. (D) Example of cluster migration producing, in this case, a trailing spiral, as seen from a top view of the mound. (E–G) Side view sequence of a cluster having reached the top of mound. As the tip rises above the mound base narrows, the cluster remains at the apex. (E) 0 minutes. (F) 14 minutes. (G) 34 minutes. Scale bars, 20 μ m.

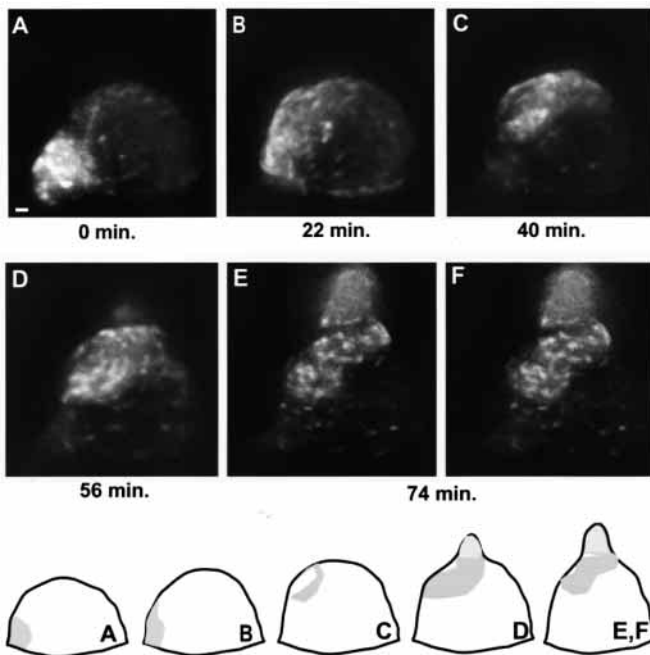



Fig. 2. Side view sequence of an ecmAO-GFP cluster rising to the top of a mound. (A) In this mound, a localized cluster first appears at the periphery of the mound base, 0 minutes. (B) Cluster migration in progress, yielding a narrow column of ecmAO-GFP cells along the left edge of the mound, 22 minutes. (C) The cluster has reached the upper half of the mound, 40 minutes. (D) Mound tip starts to form. (The tip is out-of-focus and appears as a hazy zone at the apex.) The cluster has enlarged, 56 minutes. (E,F, stereo pair) The tip elongates and is filled with labeled cells (again haze at apex, out of focus). The cluster, still larger, takes the form of a spiral (stereo pair). At this stage, most labeled cells are part of the elongate spiral, but some individual cells are still found throughout the mound base. During the period of tip formation, the number of cells exhibiting ecmAO-GFP fluorescence has increased considerably. A schematic of cluster migration and elongation is illustrated at the bottom. The identification of the cluster is based on the time-lapse movie of these data which shows that the cluster moves en masse and that cells within the cluster remain associated. Scale bars, 20 μ m.

expression in the mound not widely reported. (See Fig. 4 for a schematic and quantification of these different sorting stages.) The psA intermediate stages are largely the counterparts of the ecmAO prestalk patterns described above, and so consolidate these observations. In particular, we found that a single dark patch appeared in the mound (Fig. 3D,E, top views), and exhibited either a dark, comma-shaped pattern (Fig. 3D) or a dark vertical column (Fig. 3F, side view). Once a tip had formed, the dark zone occupied only the highest central portion of the mound including the tip (Fig. 3G-I). These dark columns

were not due to a light penetration problem through the central axis of the mound because they were never observed in mounds composed of randomly labeled cells (data not shown).

All of the preceding psA-GFP patterns appeared to be the inverse of the ecmAO prestalk patterns observed with ecmAO-GFP. However, we did observe one intermediate psA  pore pattern that was not complementary to any of the ecmAO prestalk patterns observed. This was a patchy appearance of dark regions (Fig. 3C) that emerged before the final, single dark cluster formed. In contrast, ecmAO-GFP patterns were never patchy (see also Fig. 5 below).

The ecmAO prestalk cluster forms by directional motion not differential adhesive sorting

The mechanism of prestalk cell sorting to the mound tip has been a long-standing question in *Dictyostelium* pattern

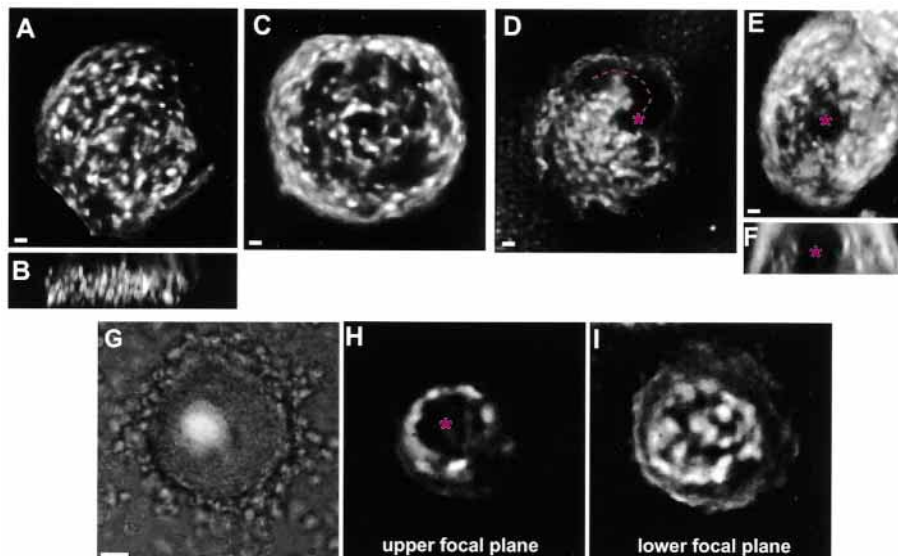


Fig. 3. Sequential intermediate stages of psA-GFP sorting in mounds. (A,B) Scattered distribution. (A) Top view. (B) Side view. (C) Intermediate sorting stage with a hint of clumped dark patches. (D) A single, large dark patch (purple *) has emerged with a comma-shaped trailing tail (purple dashed line) in top view. (E,F) A dark patch (purple *) near the mound's central axis with a trailing tail that forms a vertical dark column. (E) Top view. (F) Side view. (G-I) A later-stage mound in which the dark patch (purple *) occupies only the highest, central portion of the mound (top views). (G) Bright-field. (H) Upper focal plane. (I) Lower focal plane. Scale bars, 20 μ m.

formation. Two alternative models have been proposed: chemotactic sorting whereby prestalk cells are attracted directly to the tip or differential adhesive sorting whereby prestalk and prespore cells segregate into distinct populations based on adhesive preferences. Our results now demonstrate that prestalk sorting does not occur directly to the tip in this Ax3 strain as had been previously presumed, but rather to a random location in the mound. Nevertheless sorting does occur, and so we sought to determine how. If a guidance mechanism such as chemotaxis is operative, then prestalk cells should move directionally into the prestalk cluster. In contrast, if a sorting mechanism such as differential adhesion is operative, then cells should move randomly and accumulate in local clusters which themselves move randomly and accumulate in still larger clusters, and so on.

Our ability to follow cell movements in 3D at closely spaced time intervals has permitted us to distinguish between these two hypotheses. We examined the distribution of prestalk cells in nine different mounds as a function of time during the process of ecmAO prestalk cluster formation (see Fig. 5 for an example). It was immediately apparent that ecmAO prestalk cluster formation did not occur by the gradual accretion of cell clumps, as predicted by a differential adhesive model. During cluster formation, some ecmAO prestalk cells were observed to associate (see blue solid dot and yellow asterisk cells in Fig. 5), but these associations were always fleeting. Moreover, many ecmAO prestalk cells entered the cluster without contacting other ecmAO cells (see magenta open circle and green solid dot cells in Fig. 5). Therefore, our observations of ecmAO-GFP cluster formation are inconsistent with a model based on differential adhesive sorting.

To determine if cluster formation occurred by some

guidance mechanism, we quantified individual trajectories of ecmAO prestalk cells (nine different mounds) to look for non-random, directional motion. This trajectory analysis was complicated by the fact that, in normal mounds, directed rotational motion of all cells occurred and did not appear to be associated with cluster formation. However, in mounds with a bulk rotational flow (Fig. 6A-C), trajectories also spiraled inward suggesting that superimposed on the rotational motion, there was a specific signal attracting ecmAO-GFP cells inward to the site of ecmAO prestalk cluster formation. To test this and to evaluate cell trajectories in the absence of rotation, we mixed wild-type ecmAO-GFP cells with a mutant, myosin II regulatory light chain null (RLC⁻) cells (Chen et al., 1994), which were known to exhibit minimal rotation in the mound (Clow and McNally, 1999). We found that, even in the absence of rotation, ecmAO prestalk cells were able to form a cell cluster and that the cell trajectories once again appeared to be directed inward as they entered the cluster (Fig. 6D-F).

To confirm more rigorously that ecmAO prestalk cell trajectories exhibited inward directional motion to the site of cluster formation, we quantified the trajectory data. We reasoned that, if a guidance cue emanates from the site of cluster formation, then cells should move preferentially inward toward that site. Such directional motion would be characterized by a preponderance of movement steps toward the cluster, manifested as either an inward spiral to the cluster when rotation was present, or more linear inward movement when rotation was absent. In contrast, in the absence of a directional cue at the site of cluster formation, cell movement should be characterized by an equal number of steps toward or away from the cluster. We defined the cluster as the center of mass of those cells constituting it, and then determined how often cells moved toward or away from this site as a function of time during cluster formation. After pooling 41 tracked cells from four different mounds, we found that the percentage of steps towards the center of mass was significantly higher than random (50%), ranging anywhere from 61-88% of all steps being inward toward the cluster during the 15 minutes prior to cluster formation (Fig. 7). Nearly all of these percentages at different timepoints were highly significant, with most *P* values ranging from 0.0001 to 0.01. Curiously, between 15 and 18 minutes prior to cluster formation, we observed statistically significant outward trajectories. Directional outward motion during this 3-minute period could reflect a transient repulsion of these prestalk cells, but given its appearance exclusively in this 3-minute time interval, we are reluctant to conclude that this behavior is typical. Beyond 18 minutes, the pooled data fell below statistically significant levels suggesting that, on average, sufficiently strong directional cues are present only up to 18 minutes before an obvious cluster appears. However, in some mounds, inward directional motion can start much earlier since, in some cases, we observed statistically significant directional trajectories as early as 38 minutes prior to cluster formation. Together, these quantitative data demonstrate that motion into an ecmAO prestalk cluster is non-random, and likely reflects a response to a guidance cue at the site of cluster formation.

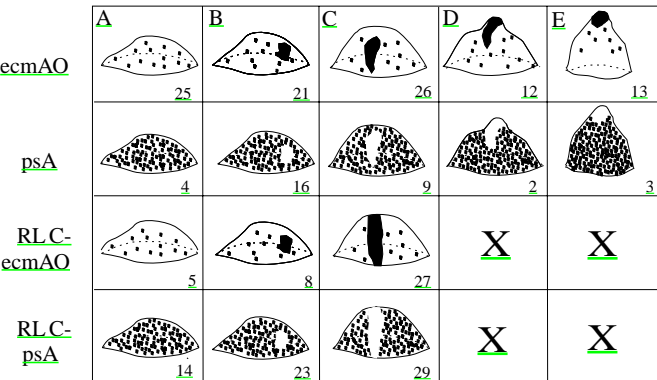


Fig. 4. Schematic and quantification of cell sorting stages for ecmAO and RLC⁻ cells. The numbers at the bottom right of each panel give the maximum number of mounds that were observed at that particular sorting stage, based either on recorded static images or on time-lapse movies of mounds. Note that these numbers do not reflect the percentage of time in each stage, but are presented only to indicate the number of examples of intermediate sorting stages that were observed. The sorting stages are defined as follows: (A) scattered, (B) elongation, (C) elongation of cluster and migration to apex, (D) arrival of cluster at tip coincident with tip formation, (E) condensation of cluster in tip and tip elongation. As observed in time-lapse movies, normal mounds never bypassed the intermediate stages (B-D). Large Xs indicate that RLC⁻ mounds arrested at stage (C) with a vertical column that failed to condense upward into a tip.

Aberrant tip formation is associated with aberrant cell sorting
The appearance of a tip only after the ecmAO prestalk cluster

reaches the mound apex suggests that upward migration of this cluster initiates tip formation. To assess this possibility, we examined the genesis and evolution of the ecmAO prestalk cluster in a mutant with aberrant tip formation. For this, we selected the myosin II regulatory light chain null (RLC⁻), a mutant that arrests at the mound without forming a tip (Chen et al., 1994).

In the RLC⁻ mutant background, we found that ecmAO-GFP

cells arrested at an intermediate stage in sorting. (See Fig. 4 for a schematic and quantification of the different sorting stages observed in this mutant.) A vertical column of ecmAO prestalk cells formed in this mutant (Fig. 8D,E, top views; F, side view), but the ecmAO cells never rose upward to condense within a nascent tip. Initially, as observed for wild-type cells, RLC⁻-ecmAO prestalk cells were scattered randomly, as seen from either a top down (Fig. 8A) or side view (Fig. 8B) of the

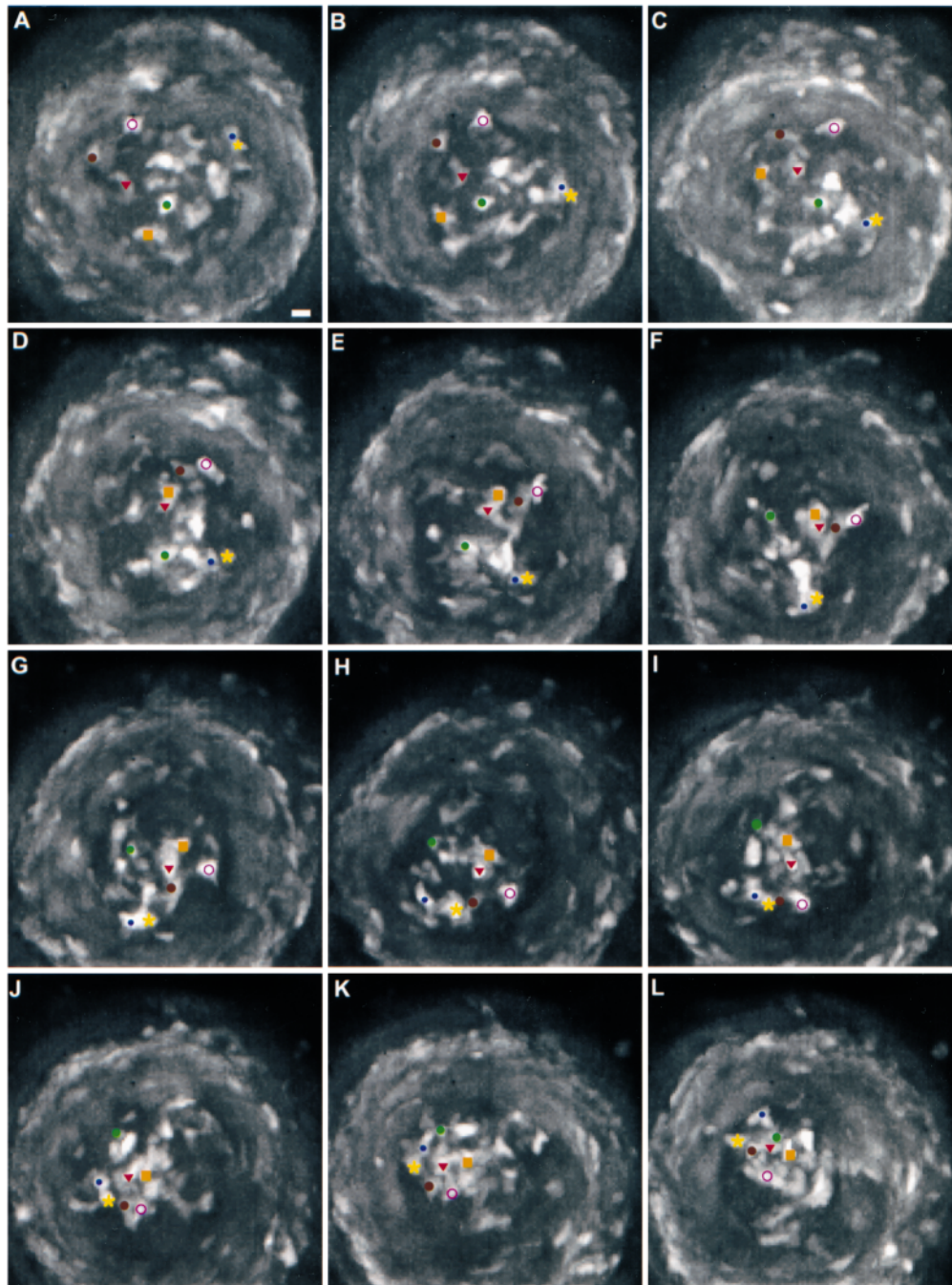


Fig. 5. Sequence of ecmAO-GFP cluster formation as seen from a top down view of one mound. Initially, the cells are scattered (A), but after 16.5 minutes have converged to form a cluster (J). During cluster formation, most cells enter the cluster independently. Isolated smaller clusters are not observed, except that sometimes two cells may form transient associations (e.g. the cells marked by the blue dot and yellow asterisk are associated from A-J, then separate). This mound exhibited clockwise rotational motion, as can be seen by following individual labeled cells. Cells that form the cluster also exhibit a net radially inward motion. Timepoints are 1.5 minutes apart. Scale bar, 10 μ m.

mound. As also observed for wild-type cells, RLC^{-} -ecmAO prestalk cells segregated to form an initial cluster at some random location within the mound. Still consistent with the behavior of wild-type cells, the cluster migrated leaving a comma-shaped trail of cells behind it (Fig. 8C, top view), which evolved into the vertical column (Fig. 8D,E, top views; F, side view), although, unlike wild-type cells, spiral staircase patterns were not observed (as in Fig. 2E,F). The absence of a spiral trail may be because all traces of rotational motion were

abolished in this mutant as the vertical column formed. In some rare RLC^{-} -mounds, a transient tip formed (Fig. 8G, top view). In the RLC^{-} -mounds, the column of ecmAO-GFP cells was always found in (Fig. 8H, top view), but still extending beneath the tip (Fig. 8I, side view). The tip eventually retracted and in no case was the column of ecmAO prestalk cells observed to condense upward.

Our observations with RLC^{-} -ecmAO-GFP cells were consolidated by observation with RLC^{-} -psA-GFP cells. These

prespore patterns in RLC^{-} -mounds were, as with wild-type mounds, largely the inverse of ecmAO prestalk patterns. In particular, sorting arrested at an intermediate stage in which a dark column lacking any psA-GFP cells formed down the central core of the RLC^{-} -mound, and this column failed to evolve any further (Fig. 9E,F). Initially, psA-GFP cells were scattered randomly within the RLC^{-} -mound, as seen from either a top view (Fig. 9A) or side view (Fig. 9B). Later, a larger dark patch appeared (Fig. 9D, purple * in top view) with a trailing comma (Fig. 9D, dotted line). Next the dark column formed, and this persisted unchanged for as long as mounds were observed (up to 12 hours). Unlike wild-type mounds, RLC^{-} -psA prespore cells never emigrated into the base and midsection of the dark column. This persistent dark column of prespore cells is the correlate of the bright ecmAO prestalk column in this mutant. In rare RLC^{-} -mounds in which a transient tip formed (Fig. 9G, top view), a dark column was still found in (Fig. 9H, top view) and beneath (Fig. 9I, top view) the tip and, as in other RLC^{-} -mounds, the column remained unchanged for hours, long after the tip retracted.

As in wild-type psA-GFP mounds (Fig. 3C), we observed an intermediate stage of multiple dark regions in RLC^{-} -psA-GFP mounds (Fig. 9C, top view). Again, there was no bright correlate in the RLC^{-} -ecmAO-GFP mounds to permit further analysis of what these clumps might represent or how they might move. Perhaps related to these dark regions, we found that even when sorting was complete, a low percentage of RLC^{-} -mounds (10-15%) exhibited 2-3 distinct dark columns (Fig. 9J, top view), instead of only one as in wild-type mounds. These dark columns appeared to arise from multiple dark patches that failed to coalesce into a larger dark patch. Comparable multiple bright columns were observed

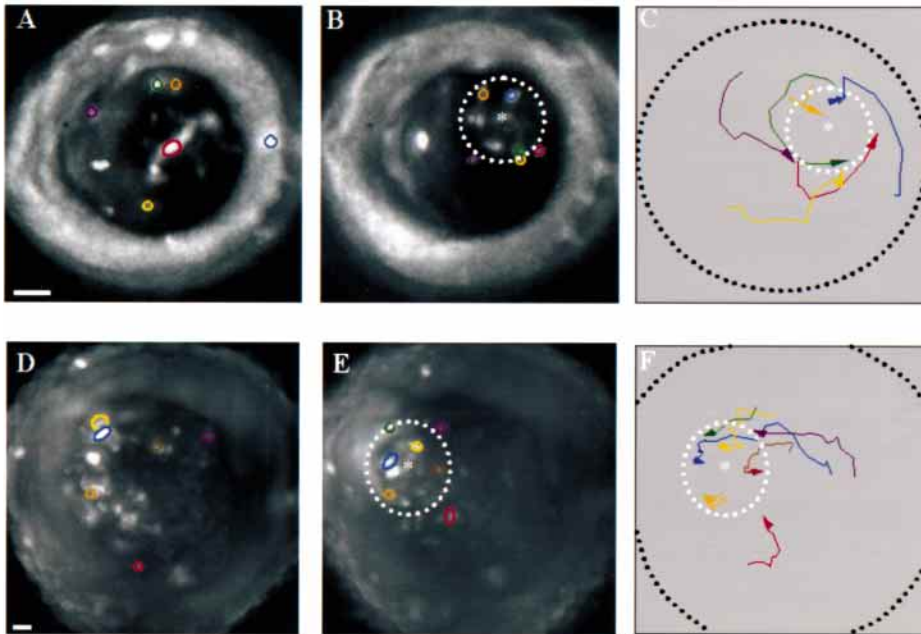


Fig. 6. Formation of an ecmAO-GFP cluster, with corresponding trajectories of marked cells. Shown are top views of two different mounds. Colored circles on cells in images match colored trajectories at right. Arrowheads indicate the endpoint of the trajectory. The white asterisk (B,C,E,F) indicates the center-of-mass of the cluster, and the dotted white line indicates the cluster's approximate boundary. The dotted black line (C,F) indicates the mound's periphery. Note that the two clusters examined here have both formed away from the mound's center point where the tip normally forms. These images have been printed at a high contrast level so that most of the cells labeled with colored circles are visible. At higher contrast levels a few other cells become visible (such as that corresponding to the purple circle in B), but most other cells disappear into a white background. Tracking of individual cells is done by setting an appropriate contrast level to visualize the cell being tracked. (A-C) Cluster formation in a mound composed entirely of wild-type cells. (A) ecmAO-GFP cells in an initial scattered distribution. (B) ecmAO-GFP cells 18 minutes after (A) in the process of cluster formation. (C) Trajectories of the six marked cells during cluster formation. Cells move directionally into the forming cluster, with the exception of the orange cell whose motion appears random. Note that the directional motion is composed of two components: rotational and inward. The inward motion is specific to cluster formation, while the rotational motion is common to all cells in these mounds. Trajectory lengths range from 21-33 minutes. (D-F) Cluster formation in a mound composed of 20% wild-type ecmAO-GFP cells plus 80% unlabeled RLC^{-} -cells. Such chimeric mounds exhibit less rotational motion, thereby minimizing the rotational component in ecmAO-GFP cell trajectories. (D) ecmAO-GFP cells in scattered distribution. (E) ecmAO-GFP cells in the process of forming a cluster. The green cell was not visible at the timepoint shown in (D), but appeared soon afterward (6.3 minutes later). Image in (E) was taken 41 minutes after (D). (F) Trajectories of seven cells in the process of forming a cluster. All cell trajectories appear highly directional toward the site of cluster formation, except the orange cell whose motion appears random. Trajectories span a range of 41-82 minutes. (Note that the enhanced outer ring of fluorescence in panels A,B is partly artifactual due to contrast enhancement. This contrast stretching amplifies a dim outer ring of fluorescence that probably arises by autofluorescence, since it can be faintly detected even in mounds composed entirely of unstained cells. Authentic cells can be distinguished as distinct blobs superimposed on this more diffuse background.) Scale bars, 40 μ m.

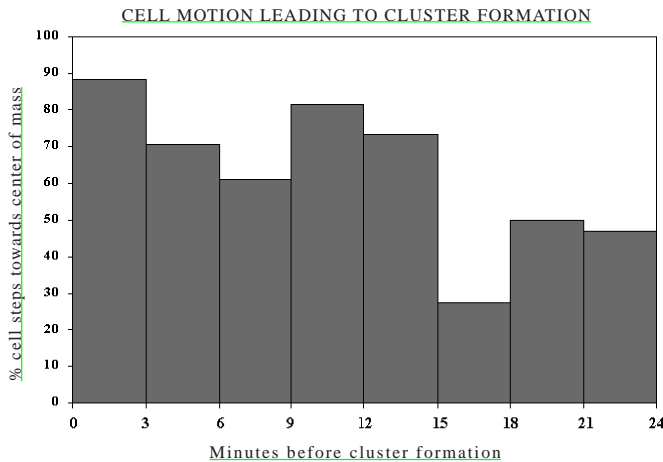


Fig. 7. Quantitative analysis of ecmAO-GFP cell motion during cluster formation. Trajectories of ecmAO-GFP cells were analyzed (see Materials and Methods) to determine the percentage of inward steps toward the site of cluster formation. This calculation was performed at 3-minute intervals during the 24 minutes prior to cluster formation. Purely random motion should yield an equal number of inward and outward steps, i.e. a 50% value for each histogram bar. For the 15 minutes prior to cluster formation, all histogram values were greater than 50%, suggesting highly non-random motion inward. The 15-18 minute bar suggests non-random motion outward. The 18-24 minute bars suggest no bias for inward or outward motion. This was confirmed by a statistical analysis based on the Gaussian approximation to the binomial probability. *P* values for each time interval were: 0-3 minutes, *P*=0.0018 (*n*=17); 3-6 minutes, *P*=0.0013 (*n*=58); 6-9 minutes, *P*=0.0675 (*n*=54); 9-12 minutes, *P*<0.0001 (*n*=54); 12-15 minutes, *P*=0.0025 (*n*=41); 15-18 minutes, *P*=0.0129 (*n*=29); 18-21 minutes, *P*=0.4168 (*n*=22); 21-24 minutes, *P*=0.5 (*n*=17). The data are derived from 41 cells from four different mounds.

with ecmAO-GFP in the RLC⁻ background (Fig. 8J,K, top views). The failure to produce a single ecmAO prestalk column in a few RLC⁻ mounds may reflect either a motile defect that prevents neighboring patches from joining, or a signaling defect that reflects an inability to establish a dominant cluster.

Aberrant sorting in RLC⁻ mounds reflects a motility defect and suggests that tip formation requires upward ecmAO prestalk cell motion

In general, the aberrant sorting of prestalk and prespore RLC⁻ cells could reflect defects in motility, signaling, or both. To test whether there were normal signals to guide cells to the tip in RLC⁻ mounds, we created chimeric mounds that contained mostly RLC⁻ cells, but included a small percentage of wild-type cells containing the ecmAO-GFP construct. In mounds with 5% wild-type cells and the remainder RLC⁻ cells, the wild-type cells expressing ecmAO-GFP moved to the tip (Fig. 10A,B, top views; C, side view). This suggests that sufficient guidance signals are still present in these predominantly RLC⁻ mounds to guide wild-type prestalk cells to the tip.

If the guidance signals in predominantly RLC⁻ mounds are sufficient for entry of wild-type cells into the tip, then this suggests that RLC⁻ prestalk cells fail to sort properly because of a motility defect. To test this, we created mounds containing a majority of wild-type cells but including a low percentage of

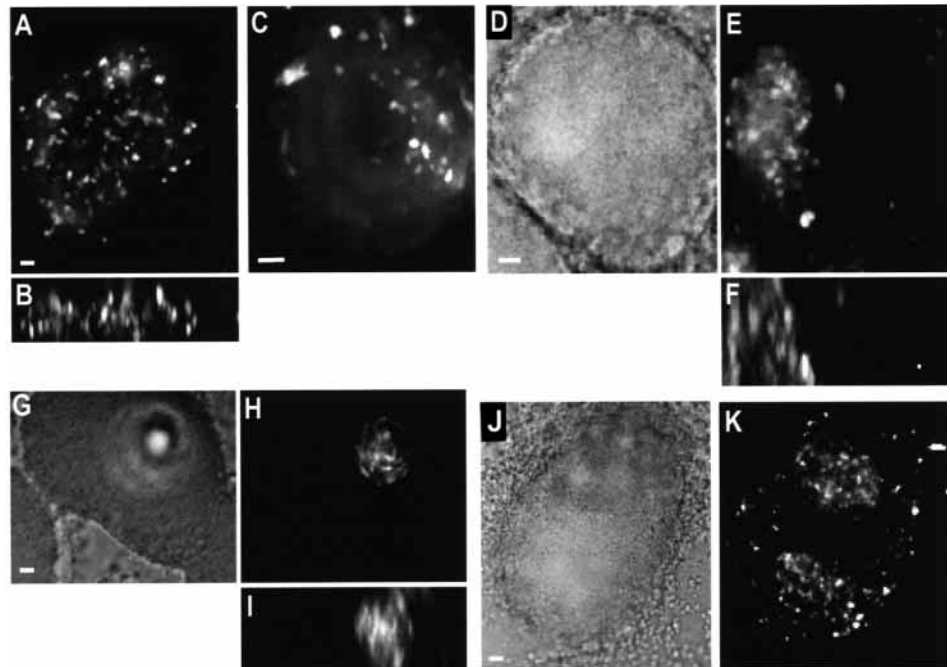
RLC⁻ cells containing ecmAO-GFP. These mounds should provide proper guidance signals, and so we predicted that RLC⁻ ecmAO-GFP cells would still show defective localization if in fact their sorting defect reflected a problem in motility. Consistent with this prediction, we found that ecmAO prestalk sorting of RLC⁻ cells was still aberrant in mounds composed of 80% wild-type cells and 20% RLC⁻ cells. In chimeric mounds, RLC⁻ cells marked with ecmAO-GFP formed a broad vertical column of cells beneath the tip, but this column never resolved to a cluster of cells localized within the tip (Fig. 10D,E, top views; F, side view). When wild-type cells were marked with ecmAO-GFP in chimeric mounds of the same proportions, GFP-labeled cells consistently localized to the tip. This demonstrates that in such chimeric mounds proper guidance signals are present, and wild-type cells respond to them. Therefore, the failure of RLC⁻ cells to condense in the tip reflects a motility defect.

A tip could form either because prestalk cells actively move upward or because other cells in the mound push them upward. The mixing experiments argue that active movement of ecmAO prestalk cells is required to form a tip. In mounds composed of 80% wild-type cells and 20% RLC⁻ cells, the RLC⁻ cells marked with ecmAO-GFP are still left in a vertical column unable to migrate into the tip (Fig. 10D,E, top views; F, side view). This presumably reflects a cell autonomous defect that cannot be overcome by movements of wild-type cells elsewhere in the mound. This hypothesis is also supported by the converse experiment in which mounds containing only 5% wild-type cells consistently produced a tip always containing a cluster of ecmAO prestalk cells (Fig. 10A,B top views; C, side view). These observations demonstrate that a small percentage of wild-type cells can sort properly and do not require the concerted movements of many other cells in the mound. Sometimes chimeric mounds composed of only 5% wild-type cells even produced elongate fingers and slugs which migrated away and left a large portion of the mound behind (Fig. 10G). Once again, wild-type cells expressing ecmAO-GFP were always in the slug tip, not in the mound left behind (Fig. 10H,I). The fact that many cells were left behind suggests that, for slug migration, the RLC is required in many cells beyond just those in the tip.

DISCUSSION

Our in vivo analysis of cell sorting in the *Dictyostelium* mound has provided the first direct evidence that guidance cues direct the sorting of ecmAO prestalk cells in normal Ax3 mounds. We found that a cluster of ecmAO prestalk cells arises at a random position in the mound via largely independent, directional movement of ecmAO prestalk cells to the site of cluster formation. ecmAO prestalk-cell motion is radially inward toward the cluster site and is superimposed on and independent of the rotational motion exhibited by both prestalk and prespore cells in the mound. Such inward-directed motion of ecmAO prestalk cells is precisely the behavior expected if these cells accumulate in response to a localized guidance cue. In contrast, we found no evidence supporting a role for differential adhesion in the initial sorting of these ecmAO prestalk cells. If ecmAO cells were sorting by differential adhesion, these cells should have moved randomly and formed

Fig. 8. Sequential stages of ecmAO-GFP sorting in an RLC-mound. (A,B) Scattered initial distribution. (A) Top view. (B) Side view. (C) Cluster migration. The head of the cluster is at the 4:00 position, followed by a curving trail of labeled cells to the 11:00 position. (D-F) Arrest of ecmAO-GFP sorting in a vertical column. (D) Bright-field top view showing the mound boundary. (E) Fluorescence top view of the ecmAO-GFP column. (F) Side view of the same column, which extends from the mound apex to its base. (G-I) A rare tipped mound. ecmAO-GFP cells also arrest in a column. (G) Bright-field top view. (H) Top view of column associated with mound tip. (I) Side view of column extending beneath mound tip. (J,K) Example of a mound with two distinct ecmAO-GFP columns (top view). (J) Bright-field. (K) ecmAO-GFP fluorescence in the same mound. Scale bars, 20 μm .



multiple, small clusters that gradually merged into a single large cluster. Instead, ecmAO cells moved independently and non-randomly to the site of cluster formation. Thus, our observations demonstrate that for ecmAO prestalk cells sorting occurs via guidance signals, not differential adhesion.

Although we found strong evidence for guidance cues in mediating ecmAO sorting, some of our data from prespore-GFP marked mounds provide hints for an adhesive component

to cell sorting. First, in psA-GFP mounds, we observed a dark central column in which psA-GFP-expressing cells were completely absent. This uniformly dark column could reflect such strong adhesion among the ecmAO prestalk cells constituting the column that psA prespore cells are absolutely excluded. Thus, adhesion among ecmAO cells could be an important factor in maintaining the integrity of the ecmAO cluster once it has formed. Second, we observed hints of

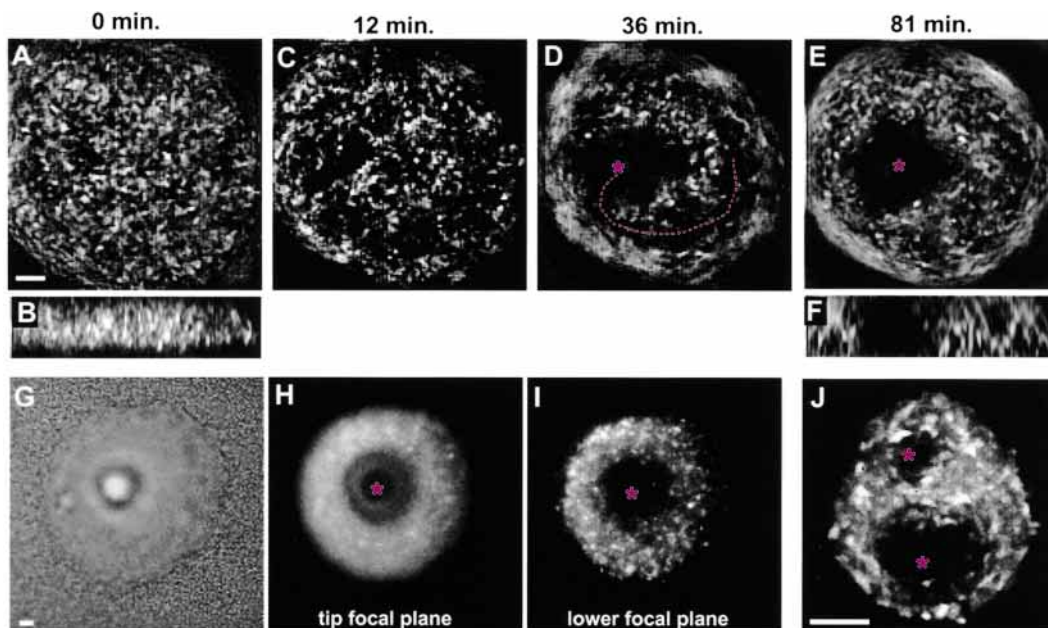


Fig. 9. Sequential stages of psA-GFP sorting in an RLC-mound. (A,B) Scattered distribution, 0 minutes. (A) Top view. (B) Side view. (C) Intermediate sorting stage exhibiting hints of several dark patches, especially from the 6:00-9:00 positions. 12 minutes. (D) Larger dark patch (purple *) with trailing tail (purple dashed line). 36 minutes. (E,F) Arrest of sorting with dark vertical column. 81 minutes. (E) Top view. (F) Side view. (G-I) A rare tipped mound with sorting arrested. A dark column still forms. (G) Brightfield top view revealing the tip, which forms transiently. (H) Top view of the dark column associated with the mound tip. (I) Side view of the dark column extending beneath the mound tip. (J) Example of a mound that exhibits two distinct dark columns (top view) delineated by the surrounding psA-GFP cells. Scale bars, 40 μm .

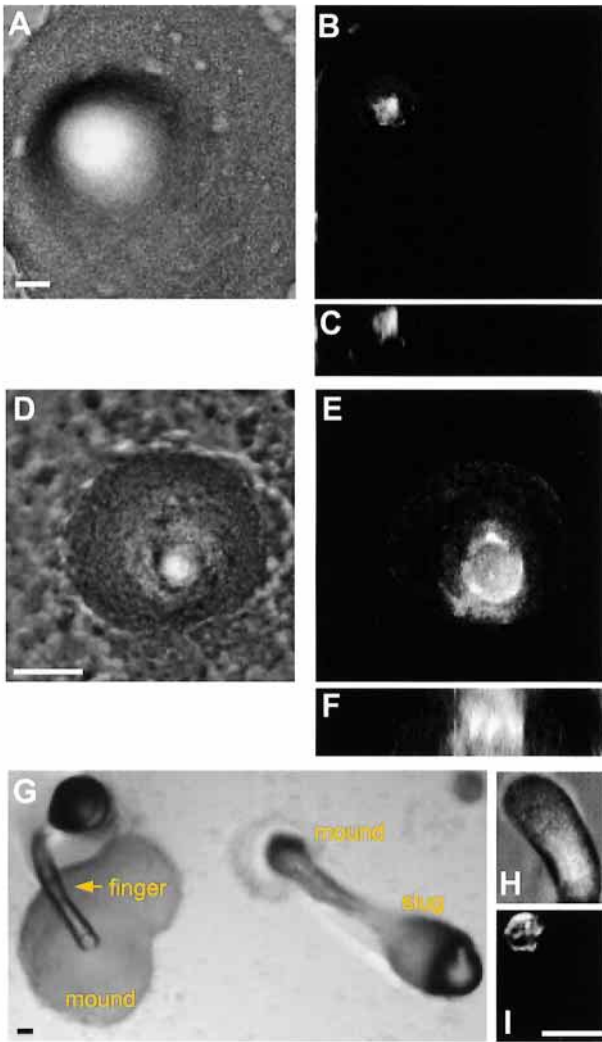


Fig. 10. Chimeric mounds exhibiting cell autonomous behavior. (A-C) Tipped mound of 5% wild-type ecmAO-GFP cells mixed with 95% unlabeled RLC⁻ cells. (A) Bright-field top view. (B,C) Wild-type ecmAO cells are in the mound tip. (B) Top view. (C) Side view. (D-F) Tipped mound of 70% RLC⁻ ecmAO-GFP cells mixed with 30% unlabeled wild-type cells. (D) Bright-field top view. (E,F) RLC⁻ ecmAO cells form a vertical column within and beneath the tip. (E) Top view. (F) Side view. (G) Bright-field image of structures resulting from mixing 10% wild-type cells with 90% RLC⁻ cells. Note the skinny finger on the left that has left the remaining cells arrested in a large mound. On the right, a slug crawls away leaving parts of the mound and finger behind. (H,I) Wild-type ecmAO prestalk cells are found at the very anterior of these renegade fingers and slugs. (H) Bright-field. (I) Fluorescence. Scale bars, 40 μ m.

multiple dark patches in mounds marked with psA-GFP. The presence of multiple dark patches implies that spore cells are being excluded from multiple sites, perhaps by clustering of some undefined subset of prestalk cells within each dark patch. According to differential adhesion, these multiple dark patches could represent intermediate cell clusters that gradually merge to form a single cluster. Alternatively, the clusters may reflect multiple chemotactic centers that mutually inhibit one another until a single site emerges. These hypotheses could be tested by examining motion of these dark

clusters, once a marker is found that provides a positive signal for cells within these clusters. Until such a marker is found, how and why these dark patches form will remain uncertain.

In addition to addressing mechanisms of cell sorting, our observations have better characterized the mechanism of tip formation and more precisely defined myosin II's role in this process. Tip formation requires myosin II, as demonstrated by the failure of several different myosin II mutants to form tips (DeLozanne and Spudich, 1987; Knecht and Loomis, 1987; Chen et al., 1994; Egelhoff et al., 1993). Myosin's function in tip formation is prestalk specific, since the myosin RLC is required only in prestalk cells for proper tip formation (Chen et al., 1998). Consistent with this prestalk requirement for myosin are observations that prestalk cell sorting is itself aberrant in another myosin mutant, namely myosin II null cells. In these mutant mounds, ecmAO cells (as assayed by β -galactosidase expression) accumulate in a central cluster (Traynor et al., 1994), reminiscent of the transient initial cluster that we observed here in normal mounds. Traynor and coworkers concluded that this cluster was the correlate of the tip, which they suggested had in some way been induced to form in the mound interior. Our in vivo studies now enable us to offer a new interpretation of these data and shed light in general on both the function of myosin in prestalk cells and the function of the prestalk cells themselves in tip formation. First, we found that the myosin II RLC is required for a myosin-dependent, cell autonomous mechanical function in prestalk cells, since small numbers of the RLC⁻ cells mixed into normal mounds still failed to move properly. Also consistent with a mechanical function, we found that a small number of normal cells in a largely RLC⁻ mound could move properly, demonstrating that RLC⁻ mounds still provide an appropriate signal to guide mechanically competent cells to the mound apex. Second, we showed that the RLC contributes to myosin-dependent mechanical function required for upward movement of the prestalk cluster. In RLC⁻ mounds, this cluster fails to condense in the forming tip. By analogy, the ecmAO clusters observed by Traynor and coworkers (1994) in myosin II null mounds could also be prestalk clusters that failed to migrate to the mound apex, rather than reflecting a new site for tip formation as they originally proposed. In normal mounds, we found that the upward movement of the prestalk cluster always led to tip protrusion as the cluster reached the mound apex. Taken together, our observations on normal and mutant Ax3 mounds therefore suggest (1) the prestalk cluster is a progenitor to the tip, (2) its upward movement normally leads to tip protrusion, (3) this upward movement requires myosin II function, and (4) tips fail to form in myosin II mutants because the prestalk cluster fails to move upward. Interestingly, this defect in *Dictyostelium* has striking parallels in *Drosophila* oogenesis where border cells migrate as a group through a surrounding mass of nurse cells (Edwards and Kiehart, 1996). Depletion of the RLC leads to arrest of border cell migration, raising the possibility that myosin II could be more generally involved in the migration of a cell cluster through a surrounding tissue.

In the course of our in vivo analysis of cell sorting, we identified several intermediate stages that have not been widely reported or appreciated in previous static analyses of prestalk gene expression patterns. We observed that an ecmAO prestalk cluster formed first at a random location in Ax3 mounds, and

then proceeded to the tip. En route to the mound apex, the cluster often grew in size as more ecmAO-expressing cells became visible and joined the cluster. These elongated clusters took the form of columns or spirals. Comparable spiral clusters have been reported in two previous studies that used either a partial ecmAO promoter (Early et al., 1995) or another prestalk enriched marker, RasD (Esch and Firtel, 1991), to drive β -galactosidase expression. Similar curved or 'comma-shaped' patterns of ecmAO expression have also been seen by β -galactosidase staining in mutant mounds that lack a particular cAMP receptor, cAR2-null cells (Saxe et al., 1996). We argue below that such 'comma-shaped' structures may be prevalent in this mutant because development either arrests or is significantly delayed at this particular intermediate sorting stage.

These in vivo observations of intermediate sorting stages raise new questions about how directional sorting of ecmAO cells occurs in an Ax3 mound. The chemotactic model for cell sorting proposes that the tip is a cAMP signaling center that attracts ecmAO prestalk cells. However, if the mound apex emits cAMP (or some other signal) to which ecmAO prestalk cells are attracted, why do these cells first congregate at another location within the mound? Our observations imply that this initial clustering is mediated by a signal that is temporally distinct and possibly qualitatively different from the signal at the mound apex. We suggest a 'twofold signaling' model (Fig. 11) in which ecmAO prestalk cells respond to the first signal (\star) by clustering at it, and then migrate largely as a unit to a second signal ($*$) at the apex. During this process of migration to the apex, new ecmAO cells continuously arise throughout the mound, and our time-lapse movies suggest they eventually join the ecmAO cluster and move coordinately with it.

This 'twofold signaling' model is readily tested by examining signaling mutants to identify those that are capable of only one step in the sorting process. According to this model, mutants unable to respond to the first clustering signal might still be capable of responding to the second apical signal. If so then, in such mutants, ecmAO prestalk cells should migrate directly and independently to the tip bypassing the initial cluster. Thus a reexamination of cell sorting patterns using ecmAO-GFP markers in a variety of signaling mutants may reveal mutants that do not form the initial ecmAO prestalk cluster. However, it is also conceivable that the initial ecmAO prestalk cluster is required for cells to be able to respond to the second signal. If so then, in mutants which do not respond to the first signal, ecmAO prestalk cells may simply remain scattered. A candidate for such a mutant may be mounds lacking tipA, a novel cytoplasmic protein, which arrest development with very small clusters of ecmAO prestalk cells (Stege et al., 1997).

According to a 'twofold-signaling' model, mutants unable to respond to the second apical signal may still form an ecmAO prestalk cluster, but the cluster should not migrate properly to the mound apex. In such mutants, β -galactosidase staining should reveal an arrested cluster of ecmAO prestalk cells. As noted already, one candidate for such a mutant are cells lacking a specific cAMP receptor, namely cAR2. cAR2⁻ cells sometimes form 'comma-shaped' ecmAO prestalk clusters (Saxe et al., 1996) suggesting that this mutant may be delayed for an extended period at this intermediate sorting stage. If this interpretation is correct, then it suggests that cAMP could play

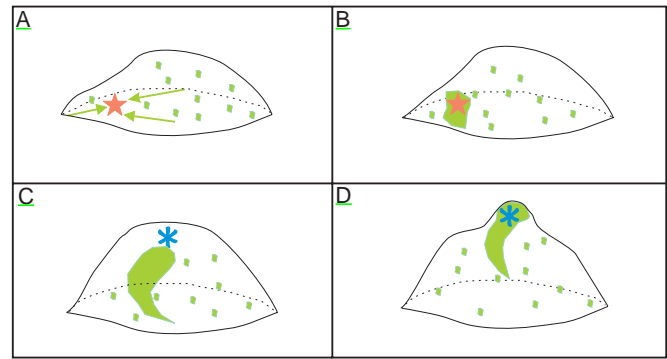


Fig. 11. Two-fold signaling model. Schematic side view of the mound. (A) ecmAO prestalk cells move directionally (arrows) towards the first signal (\star). (B) ecmAO prestalk cells have formed a single cluster at the site of the initial signal. During this period, other ecmAO prestalk cells have begun to differentiate at scattered positions throughout the mound. (C) More ecmAO prestalk cells join the initial cluster, which grows to be columnar or spiral-shaped. Still other ecmAO prestalk cells continue to differentiate at scattered positions throughout the mound. Prior to tip formation, the ecmAO prestalk cluster moves as a unit apically towards the second signal ($*$) located at the mound apex. In order to permit the cluster to form first, and then proceed to the apex, the first and second signals must be in some way distinct. The model illustrated here depicts one possibility, namely two different signals that are also separated in time. Two other scenarios are also consistent with the current data. If the two signals are different, then both could be present simultaneously, and cells may only become sensitive to the second signal after the cluster has formed. In this version of the model, the $*$ would also be present at the mound apex in A and B. An alternate possibility arises if the two signals are the same, but temporally distinct. In this version of the model, the $*$ in C and D would be replaced by a \star . (D) Part of the ecmAO prestalk cluster has reached the mound apex. Continued upward movement of the cluster leads to protrusion of the tip on the mound.

a role in directing the prestalk cluster to the mound apex (i.e. cAMP may be a component of the second signal $*$ in the model of Fig. 11). Of course, arrested prestalk clusters could also arise due to motility defects, as both we and Traynor et al. (1994) observed in cells with defective myosin II.

It is important to emphasize in closing that our studies have been performed in one of the two widely used *Dictyostelium* strains, Ax3. The other commonly used strain, Ax2, shows grossly similar morphogenetic behavior to Ax3, but previous comparisons of cell motion in mounds of the two strains have revealed some significant differences (Kellerman and McNally, 1999). Most notably, the rotational motion of cells in Ax3 mounds is absent in Ax2 mounds, and replaced by radially inward and upward motion. Since cell motion is so different between these strains, it is also possible that cell sorting patterns are also different, at least in some ways. In particular, as previously hypothesized (Kellerman and McNally, 1999), the radially inward and upward motion of Ax2 cells in the mound could reflect direct and independent sorting of prestalk cells to the tip. Thus, it will be interesting from a comparative standpoint to repeat our studies of cell sorting in Ax2. However, regardless of how Ax2 sorting may occur, our previous studies also suggest remarkable developmental plasticity between strains. By adjustment of buffering

conditions and humidity, we found that strain behavior was essentially interchangeable, and so likely reflects the extensive regulative capacity of the organism (Kellerman and McNally, 1999).

In summary we propose that sorting of ecmAO prestalk cells in *Dictyostelium* Ax3 mounds involves two distinct signals, one (★) that guides cells to the initial ecmAO cluster (Fig. 11A,B) and a second (*) that directs the migration of this cluster to the apex (Fig. 11C). As the cluster reaches the mound apex, its continued upward movement leads to tip protrusion (Fig. 11D). This active upward movement of the ecmAO prestalk cluster requires myosin II.

REFERENCES

- Aubry, L. and Firtel, R. (1999). Integration of signaling networks that regulate *Dictyostelium* differentiation. *Ann. Rev. Cell Dev. Biol.* **15**, 469-517.
- Awasthi, A., Doolittle, K. W., Parulkar, G. and McNally, J. G. (1994). Cell tracking using a distributed algorithm for 3D-image segmentation. *Bioimaging* **1**, 98-112.
- Burdine, R. D., Sands, S. and Stern, M. J. (1998). EGL-17 (FGF) expression mediates the attraction of the migrating sex myoblasts with vulval induction in *C. elegans*. *Development* **125**, 1083-1093.
- Chen, E. B. and Stern, M. J. (1998). Understanding cell migration guidance: lessons from sex myoblast migration in *C. elegans*. *Trends Genet.* **14**, 322-327.
- Chen, P., Ostrow, B. D., Tafuri, S. R. and Chisnoim, R. L. (1994). Targeted disruption of the *Dictyostelium* RMLC gene produces cells defective in cytokinesis and development. *J. Cell Biol.* **127**, 1933-1944.
- Chen, T.-L. L., Wolf, W. A. and Chisholm, R. L. (1998). Cell type-specific rescue of myosin function during *Dictyostelium* development requires two distinct cell movements required for culmination. *Development* **125**, 3895-3903.
- Clark, R., Retzinger, G. S. and Steck, T. L. (1980). Novel morphogenesis in Ax-3 mutant strain of the cellular slime mould *Dictyostelium discoideum*. *J. Gen. Microbiol.* **121**, 319-331.
- Clow, P. A. and McNally, J. G. (1999). In vivo observations of myosin II dynamics support a role in rear retraction. *Mol. Biol. Cell* **10**, 1309-1323.
- Conchello, J. A. and McNally, J. G. (1996). Fast regularization technique for expectation maximization algorithm for optical sectioning microscopy. *Proc. IS&T/SPIE Symposium on Electronic Imaging: Science and Technology, San Jose, CA 2655*, 199-208.
- DeLozanne, A. and Spudis, J. A. (1991). Disruption of the *Dictyostelium* myosin heavy chain gene by homologous recombination. *Science* **236**, 1086-1091.
- Doolittle, W., Reddy, I. and McNally, J. G. (1995). 3D analysis of cell movement during normal and myosin-II-null cell morphogenesis in *Dictyostelium*. *Dev. Biol.* **167**, 118-129.
- Durston, A. J. and Clark, F. (1979). A cinematographical study of the development of vitally stained *Dictyostelium discoideum*. *J. Cell Sci.* **36**, 261-279.
- Early, A., Firtel, R. T. and Williams, J. (1995). Evidence for positional differentiation of prestalk cells and for a morphogenetic gradient in *Dictyostelium*. *Cell* **83**, 91-99.
- Edwards, K. A. and Kiehl, D. (1996). *Drosophila* nonmuscle myosin II has multiple essential roles in imaginal disc and egg chamber morphogenesis. *Development* **122**, 1499-1511.
- Egelhoff, T. T., Lee, R. J. and Spudis, J. A. (1990). *Dictyostelium* myosin heavy chain phosphorylation sites regulate myosin filament assembly and localization in vivo. *Cell* **75**, 363-371.
- Escalante, R. and Loomis, W. F. (1991). Whole-mount *in situ* hybridization of cell-type-specific mRNAs in *Dictyostelium*. *Dev. Biol.* **171**, 262-266.
- Esch, R. K. and Firtel, R. A. (1991). cAMP and cell sorting control the spatial expression of a developmentally essential cell-type-specific *ras* gene in *Dictyostelium*. *Genes Dev.* **5**, 9-21.
- Feinberg, A. P., Springer, W. F. and Aronides, S. H. (1979). Segregation of pre-stalk and pre-spore cells of *Dictyostelium discoideum*: observations consistent with selective cell cohesion. *Proc. Natl. Acad. Sci. USA* **76**, 3977-3981.
- Godt, D. and Tepass, U. (1998). *Drosophila* oocyte localization is mediated by differential cadherin-based adhesion. *Nature* **395**, 387-391.
- Gross, J. D. (1991). Developmental decisions in *Dictyostelium discoideum*. *Microbiol. Rev.* **55**, 330-351.
- Haberstroh, J. and Firtel, R. A. (1990). A spatial gradient of expression of a cAMP-regulated prespore cell-type-specific gene in *Dictyostelium*. *Genes Dev.* **4**, 596-612.
- Heim, R., Fisher, J. C. and Tsien, R. Y. (1994). Wavelength mutations and posttranslational auto-oxidation of green fluorescent protein. *Proc. Natl. Acad. Sci. USA* **91**, 12501-12504.
- Jermyn, K. A. and Williams, J. G. (1991). An analysis of culmination in *Dictyostelium* using prestalk and stalk-specific cell autonomous markers. *Development* **111**, 779-787.
- Kellerman, K. A. and McNally, J. G. (1999). Mound-cell movement and morphogenesis in *Dictyostelium*. *Dev. Biol.* **208**, 416-29.
- Keynes, R. and Coolidge, M. W. (1995). Chemotactic guidance molecules. *Cell* **83**, 161-169.
- Knecht, D. and Loomis, W. F. (1987). Antisense RNA inactivation of myosin heavy chain gene expression in *Dictyostelium discoideum*. *Science* **236**, 1081-1086.
- Kose, H., Kose, D., Tanaka, X. and Chiba, A. (1997). Homophilic synaptic target recognition mediated by immunoglobulin-like cell adhesion molecule Fasciclin III. *Development* **124**, 4143-4152.
- Krasnow, M. A. (1997). Genes that control cell form: lessons from bone and branching morphogenesis. *Cold Spring Harb. Symp. Quant. Biol.* **62**, 235-240.
- Lam, T. Y., Mookerjee, G., Geltosky, J. and Siu, C. H. (1981). Differential cell cohesion expressed by prespore and prestalk cells of *Dictyostelium discoideum*. *Differentiation* **20**, 22-28.
- Loomis, W. F. (1971). Sensitivity of *Dictyostelium discoideum* to nucleic acid analogues. *Exp. Cell Res.* **64**, 484-486.
- Loomis, W. F. (1993). Local inhibition and pattern formation in *Dictyostelium*. *Curr. Top. Dev. Biol.* **28**, 1-46.
- Loomis, W. F. (1996). Genetic networks that regulate development in *Dictyostelium* cells. *Microbiol. Rev.* **60**, 133-150.
- Manstein, D. J., Titus, M. A., DeLozanne, A. and Audich, J. A. (1989). Gene replacement in *Dictyostelium*: generation of myosin null mutants. *EMBO J.* **8**, 923-932.
- Matsukura, S. and Dworkin, A. J. (1979). Chemotactic cell sorting in *Dictyostelium discoideum*. *J. Embryol. Exp. Morph.* **50**, 243-251.
- Mee, J. D., Tortorella, C. and Coukell, M. B. (1996). Chemotaxis as a regulated property of separated prestalk and prespore cells. *Biochem. Cell Biol.* **64**, 722-732.
- McNally, J. G., Preza, C., Conchello, J. A. and Thomas, L. J. (1994). Artifacts in computerized optical sectioning microscopy. *J. Opt. Soc. Am. [A]* **11**, 1056-1067.
- Noegel, A. and Schleicher, M. (2000). The actin cytoskeleton of *Dictyostelium*: a story from mutants. *J. Cell Sci.* in press.
- Nose, A., Nagafuchi, A. and Takeichi, M. (1988). Expression of recombinant cadherins mediate cell sorting in model systems. *Cell* **54**, 993-1001.
- Nose, A., Umeda, T. and Takeichi, M. (1997). Neurofascin cell adhesion molecules in *Drosophila*. *Development* **124**, 1433-1441.
- Preza, C., Miller, M. L., Thomas, L. J. and McNally, J. G. (1992). Regularized linear method for reconstruction of three-dimensional microscopic objects from optical sections. *J. Opt. Soc. Am. [A]* **9**, 219-228.
- Saxe, C., Yu, Y., Jones, C., Bauman, A. and Haynes, C. (1996). The cAMP receptor type cAMP restricted to a subset of prestalk cells during *Dictyostelium* development and displays unexpected DIF-1 responsiveness. *Dev. Biol.* **174**, 202-213.
- Shelton, C. A., Wilson, C. J., Ellis, G. C. and Bowerman, B. (1999). The nonmuscle myosin regulatory light chain gene *mhc-4* is required for cytokinesis, anterior-posterior polarity, and body morphology during *Caenorhabditis elegans* embryogenesis. *J. Cell Biol.* **146**, 439-451.
- Siu, C.-H., Des Roches, B. and Lam, T. Y. (1981). Involvement of cell-surface glycoprotein in the cell-sorting process of *Dictyostelium discoideum*. *Proc. Natl. Acad. Sci. USA* **78**, 6596-6600.
- Snedecor, G. W. and Cochran, G. (1980). *Statistical Methods*. 7th ed. Ames, IA: Iowa State Univ. Press.
- Speicher, S., García-Alonso, L., Carrón, A., Martín-Bermudo, M. D., de la Escalera, S. and Jiménez, F. (1998). Neurotactin functions in concert with other identified CAMs in growth cone guidance in *Drosophila*. *Neuron* **20**, 221-233.

- Spudich, J. A.** (1982). *Dictyostelium discoideum*: methods and perspectives for study of cell motility. *Methods Cell Biol.* **25 Pt. B**, 359-364.
- Steger, J. T., Shaulsky, G. and Loomis, W. F.** (1997). Sorting of the initial cell type in *Dictyostelium* is dependent on the tipA gene. *Dev. Biol.* **185**, 34-41.
- Steinberg, M. S.** (1962). Mechanism of tissue reconstruction by dissociated cells. II. Time-course of events. *Science* **137**, 762-763.
- Steinberg, M. S.** (1970). Does differential adhesion govern self-assembly processes in histogenesis? Equilibrium configurations and the emergence of a hierarchy among populations of embryonic cells. *J. Exp. Zool.* **173**, 395-434.
- Steinberg, M. S. and Poole, T. J.** (1981). Cellular adhesive differentials as determinants of morphogenetic movements and organ segregation. In *Developmental Order: Its Origin and Regulation* (ed. S. Subtelny and P. B. Green), pp. 351-378. New York: Alan R. Liss.
- Steinberg, M. and Takeuchi, M.** (1994). Experimental specification of cell sorting, tissue spreading, and specific spatial patterning by quantitative differences in cadherin expression. *Proc. Natl. Acad. Sci. USA* **91**, 206-209.
- Sternfeld, J. and David, C. N.** (1981). Cell sorting during pattern formation in *Dictyostelium*. *Differentiation* **20**, 10-21.
- Sutherland, D., Samakovlis, C. and Gasne, M. A.** (1996). branchless encodes a *Drosophila* FGF homolog that controls tracheal cell migration and the pattern of branching. *Cell* **87**, 1091-1101.
- Takeuchi, I., Iakutani, T. and Tasaka, M.** (1988). Cell behavior during formation of prestalk/prespore pattern in submerged agglomerates of *Dictyostelium discoideum*. *Dev. Genet.* **9**, 607-614.
- Traynor, D., Kesel, R. H. and Williams, J.** (1992). Chemotactic sorting to cAMP in the multicellular stages of *Dictyostelium* development. *Proc. Natl. Acad. Sci. USA* **89**, 8303-8307.
- Traynor, D., Tasaka, M., Takeuchi, I. and Williams, J.** (1994). Aberrant pattern formation in myosin heavy chain mutants of *Dictyostelium*. *Development* **120**, 551-601.
- Uyeda, T. Q. P. and Fries, M.** (1997). The myosins of *Dictyostelium*. In *Dictyostelium: A Model System for Cell and Developmental Biology* (ed. Y. Maeda, K. Inoué, and I. Takeuchi), pp. 43-64. Tokyo: Universal Academy Press.
- Wang, M. and Schaap, P.** (1985). Correlations between tip dominance, prestalk/prespore pattern, and cAMP-relay efficiency in slugs of *Dictyostelium discoideum*. *Differentiation* **30**, 7-14.
- Williams, J. G., Coffey, K. T., Lane, D. P., McFadden, S. J., Harwood, A. J., Traynor, D., Kay, R. and Jernigan, K. A.** (1989). Origins of the prestalk-prespore pattern in *Dictyostelium* development. *Cell* **59**, 1157-1163.
- Zimmerman, T. and Siegert, F.** (1998). 4D confocal microscopy of *Dictyostelium discoideum* morphogenesis and its presentation on the Internet. *Dev. Genes Evol.* **208**, 411-420.